

MicroRNA profiling of different exercise interventions for alleviating skeletal muscle atrophy in naturally aging rats

Jiling Liang, Hu Zhang, Zhengzhong Zeng, Jun Lv, Jielun Huang, Xiaowen Wu, Minghui Wang, Jiahao Xu, Jingjing Fan & Ning Chen* 

Tianju Research and Development Center for Exercise Nutrition and Foods, Hubei Key Laboratory of Exercise Training and Monitoring, College of Health Science, Wuhan Sports University, Wuhan, Hubei, China

Abstract

Background Exercise is an affordable and practical strategy to alleviate several detrimental outcomes from the aging process, including sarcopenia. The elucidation of molecular mechanisms to alleviate sarcopenia is one of the most important steps towards understanding human aging. Although microRNAs (miRNAs) regulate muscle growth, regeneration and aging, the potential role of exercise-mediated miRNAs during the prevention and rehabilitation of skeletal muscle atrophy upon exercise interventions remains unclear.

Methods A miRNA profile by miRNA sequencing for gastrocnemius muscle of a 24-month-old aged male rat model mimicking the naturally aging process was established through screening the differentially expressed miRNAs (DEMs) for alleviating aging-induced skeletal muscle atrophy upon optimal exercise intervention. The screened miRNAs and hub genes, as well as biomarkers with the most significantly enriched pathways, were validated by quantitative real-time polymerase chain reaction and western blotting.

Results The sarcopenia index (SI) value and cross-sectional area (CSA) of rats from the old control (OC) group significantly decreased when compared with the youth control (YC) group ($P < 0.001$, $P < 0.01$), whereas an increased SI value and an enlarged CSA of rats from the old-aerobic exercise (OE), old-resistance exercise (OR) and old-mixed exercise (OM) groups were determined ($P < 0.01$, $P < 0.001$, $P < 0.05$; $P < 0.01$, $P < 0.01$, $P < 0.05$). Our results demonstrate that 764 known miRNAs, 201 novel miRNAs and 505 miRNA–mRNA interaction networks were identified to be related to aging-induced muscular atrophy. Among them, 13 miRNAs were differentially expressed ($P < 0.05$ and $\log_2|\text{fold change}| > 1$) between the YC group and the OC group. Compared with the OC group, 7, 2 and 11 miRNAs were differentially expressed in the OE, OR and OM groups after exercise interventions, respectively. Meanwhile, Gene Ontology (GO) and Kyoto Encyclopedia of Genes and Genomes (KEGG) analyses revealed that the identified DEMs were primarily related to apoptosis, autophagy and the NF- κ B/MuRF1 signalling pathways ($P < 0.05$). Meanwhile, four DEMs (miR-7a-1-3p, miR-135a-5p, miR-151-5p and miR-196b-5p), six hub genes (*Ar*, *Igf1*, *Hif1a*, *Bdnf*, *Fak* and *Nras*) and several biomarkers (LC3, Beclin1, p62, Bax, Bcl-2 and NF- κ B/MuRF1) with the most significantly enriched pathways were confirmed, which may play a key role in muscular atrophy during the aging process.

Conclusions These findings are closely correlated with the progression of sarcopenia and could act as potential biomarkers for the diagnosis and interventional monitoring of aging-induced skeletal muscle atrophy.

Keywords exercise intervention; microRNA; miRNA sequencing; sarcopenia; skeletal muscle atrophy

Received: 6 July 2022; Revised: 6 October 2022; Accepted: 3 November 2022

*Correspondence to: Ning Chen, Tianju Research and Development Center for Exercise Nutrition and Foods, Hubei Key Laboratory of Exercise Training and Monitoring, College of Health Science, Wuhan Sports University, Wuhan 430079, Hubei, China. Email: nchen510@gmail.com

Jiling Liang and Hu Zhang equally contributed to this work.

Introduction

With the rapid progression of population aging, the annual incidence of sarcopenia is gradually increasing, and the number of global sarcopenia patients is expected to exceed 500 million by 2050.¹ Sarcopenia as a progressive loss of skeletal muscle mass and function can result in reduced physical activity, poor quality of life, impaired cardiopulmonary function and increased incidence of falls, disability and death for the elderly, as well as a burden from medical care and nursing.² The aetiology of sarcopenia is complex, with the involvement of multiple factors related to aging, oxidative stress, decreased hormone level, less physical activity, uneven protein homeostasis, imbalanced autophagy and apoptosis, mitochondrial dysfunction and a low number of satellite cells in skeletal muscle.³ Meanwhile, microRNAs (miRNAs) also play a critical role in the growth and metabolism of skeletal muscle cells through specifically binding to the 3'-untranslated region (3'-UTR) of target mRNAs and regulating the expression of corresponding genes related to skeletal muscle growth and metabolism at the post-transcriptional level.⁴ Furthermore, changes in miRNA expression and gene targets are associated with aging-induced alteration in skeletal muscle function and mass.⁵

However, the pathogenesis and prevention of aging-related muscular atrophy primarily focus on the relationship between exercise intervention and its efficacy. Conversely, the molecular mechanisms, such as epigenetics for sarcopenia upon exercise interventions, remain unclear. As a consequence of aging and sedentary lifestyles, elderly people may lose muscle mass more quickly.⁶ Exercise is beneficial for delaying aging-induced decline in skeletal muscle mass and functionality through the regulation of miRNAs.⁷ As an essential part of exercise adaptation to skeletal muscle, exercise-mediated miRNAs can reduce oxidative stress, enhance mitochondrial quality control, promote protein metabolism and regulate the signal pathways involved in skeletal muscle regeneration during the aging process.⁸

In the past few years, Illumina sequencing technology has been used to explore the pathogenesis and screen biomarkers, which are crucial for the diagnosis, treatment and prognostic prediction of chronic diseases. However, the underlying mechanisms for the interaction between miRNAs and sarcopenia upon exercise interventions remain unknown. In this study, a naturally aging rat model with skeletal muscle atrophy was established. The Illumina NovaSeq 6000 platform was employed to analyse the differentially expressed miRNAs (DEMs) in response to exercise interventions during aging-induced muscular atrophy. Gene Ontology (GO) function annotation, Kyoto Encyclopedia of Genes and Genomes (KEGG) analysis and the Cytoscape software for protein-protein interaction (PPI) and miRNA-mRNA interaction network analysis further screened the hub genes. Finally, the DEMs and hub genes were confirmed by quantitative

real-time polymerase chain reaction (qRT-PCR) and western blot to elucidate the molecular mechanisms of exercise interventions for delaying aging-induced muscular atrophy, thus providing new insights for the prevention, treatment and rehabilitation of sarcopenia.

Materials and methods

Animals and study design

Six-month-old Wistar male rats (body weight, 490 ± 50 g at the beginning of the experiment; Certificate No. 42000600020738) were purchased from the Experimental Animal Center at the Hubei Provincial Center for Disease Control and Prevention (Wuhan, China). Experimental procedures involving animals were carried out according to the ethical standards of the Animal Care and Use Committee at Wuhan Sports University. All rats were reared with free access to food and water and randomly divided into four groups: the naturally aging rats as the old control (OC) group, the old rats subjected to aerobic exercise as the old-aerobic exercise (OE) group, the old rats subjected to resistance exercise as the old-resistance exercise (OR) group and the old rats subjected to aerobic exercise combined with resistance exercise as the old-mixed exercise (OM) group, with six rats in each group. Following the successful construction of the naturally aging model, six 6-month-old male Wistar rats were purchased and used as the youth control (YC) group.

Exercise protocol

The aerobic exercise protocol in the Bedford study was used as a reference.⁹ The rats performed aerobic exercise on a treadmill with a slope of 10° for 12 weeks. During the first week, all rats from the OE group were engaged in treadmill running to adapt to the experimental environment, with an initial running speed of 4.2 m/min and increments of 1 m/min every 30 s until reached a running duration of 50 min/day at a speed of 12 m/min. Then, the rats from the OE group were subjected to treadmill running at a speed of 12 m/min for 50 min/day and 5 days/week, after the habituation period. As previously mentioned, the loaded ladder-climbing training was conducted as the resistance exercise.¹⁰ Initially, a 1-week habituation period was introduced, with the loaded weight of 10% of the rat's body weight as the initial loading amount. After adaptive training for 1 week, the rats were started with a loading amount of 20% of their body weight. The loading was gradually increased by 10% each week until reached the maximum loading amount of 60% of their body weight in the 5th week to the completion of resistance exercise training in the 12th week. Each animal performed nine dynamic movements per

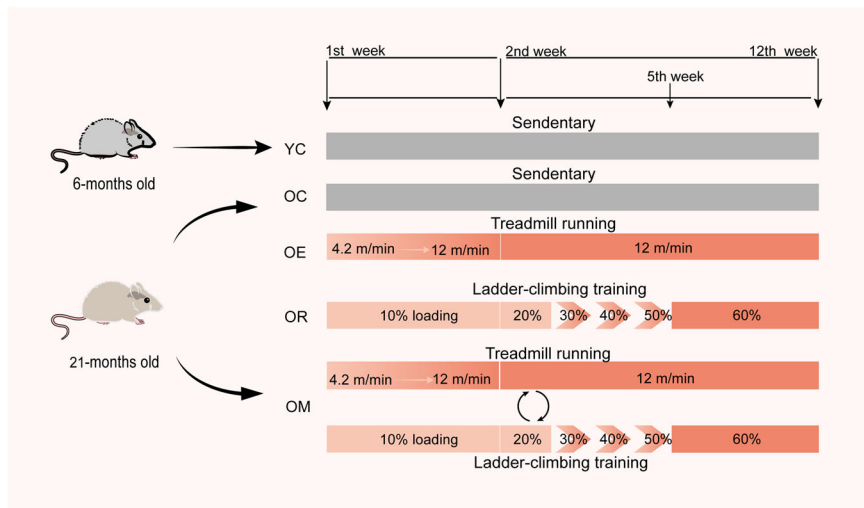


Figure 1 Schematic diagram illustrating the animal age and grouping, and exercise intervention protocols. OC, old control; OE, old-aerobic exercise; OM, old-mixed exercise; OR, old-resistance exercise; YC, youth control

climbing consisting of three sets with three repetitions, followed by 1-min rest between each repetition and 2-min rest between each set. A total of 27 exercise sessions were performed 3 days/week. The rats from the OM group alternated between treadmill running and ladder climbing with the similar training programmes to OE and OR groups every other day (Figure 1).

Sarcopenia index

The body weights of the 24-month-old rats were measured after their 12-week exercise training programme. Then all rats were sacrificed under the anaesthesia with the intraperitoneal injection of pentobarbital sodium at a dosage of 50 mg/kg. The gastrocnemius muscle in the left and right hind limbs of the rats was harvested and weighed. The skeletal muscle tissues were immediately frozen in liquid nitrogen and preserved at -80°C for subsequent use. The sarcopenia index (SI) was presented as a gastrocnemius muscle weight/body weight (GMW/BW) ratio to determine whether the model of sarcopenia was successful.¹¹ When the SI value of the rats from the aging group was significantly lower than that of the young group and the difference was more significant than 2 times standard deviation (SD), sarcopenia was indicated.

Histological examination of gastrocnemius muscle

The samples of the gastrocnemius muscle were harvested, fixed in 10% neutral-buffered formalin and sliced into 5-mm slices with a cryotome. Haematoxylin–eosin (HE) staining

was performed to assess the morphology and damage of the gastrocnemius muscle after dewaxing and rehydration. Tissue staining was quantified with three rats per group. At least three images of each tissue section were captured using a light microscope (BX51TF, OLYMPUS, Japan), and each slice in each group was observed at $\times 200$ magnification. An appropriate field of view was selected with ImageJ (National Institutes of Health, Bethesda, MD, USA) with careful manual annotation. Approximately 60–80 muscle fibres (pieces) per image were counted. At least 180 skeletal muscle fibres were counted in each group for quantification. Different regions were randomly selected in a blind mode for fibre analysis. The cross-sectional area (CSA) was measured in μm^2 using the free-hand trace tool. The total fibre count was computed using the multi-point tool, all within the software. The total area of the muscle fibres (μm^2) was measured. The number of muscle fibres (pieces) in each slice was counted. The average CSA of gastrocnemius muscle fibres (μm^2) was computed using the formula: total muscle fibre area (μm^2)/number of muscle fibres.

MicroRNAs sequencing and data analysis

According to the manufacturer's instructions, the total RNA was extracted using the Total RNA Extractor (Trizol) kit (B511311, Sangon, China). Each RNA sample was divided into five fractions with equal amounts. Three RNA samples were collected from each experimental group, namely, YC, OC, OE, OR and OM groups. In order to generate sequencing libraries for Illumina® (New England Biolab Inc., Ipswich, MA, USA), the NEBNext® Multiplex Small RNA Library Prep Set (Invitrogen, Life Technologies, Carlsbad, CA, USA) for

Illumina® was used. RNA samples containing 2 µg of total RNA from each group were directly connected to adapters, followed by reverse transcription and cDNA synthesis. The cDNA library was constructed by electrophoresizing 140–150 bp fragments of DNA. The Qubit® DNA Assay Kit (Invitrogen, Life Technologies) was used to assess the quality of the libraries, which were then sequenced using an Illumina NovaSeq 6000 (Illumina, TX, USA).

Data analysis was conducted sequentially by removing adapters using the Cutadapter v1.14 software. Trimmomatic v0.36 was then employed to trim the low-quality (quality score < 20) bases from both the 3' and 5' ends. FastQC was used to evaluate the base quality of the raw small RNA sequencing reads prior to mapping them on the reference genome. The mirDeep2 software (v2.0.0.8) was then used to quantify known miRNAs and predict novel miRNAs. In order to determine miRNAs with differential expression, P value < 0.05 and $\log_2|\text{fold change}| > 1$ were considered.

Target gene prediction, gene functional analysis and protein–protein interaction network

The target mRNAs of each miRNA were predicted using three independent online target prediction databases: TargetScan (<http://www.targetscan.org/>), miRWalk (<http://mirwalk.umm.uni-heidelberg.de/>) and miRDB (<http://www.mirdb.org/>). Then, the functional enrichment was analysed using the DAVID online tool. Following these steps, GO analysis and KEGG pathway enrichment analysis were performed with the R programming language via the clusterProfiler package (v3.0.0) for analysing the biological functions of differentially expressed genes (DEGs). The P value < 0.05 was considered to be statistically significant.

Subsequently, the Search Tool for the Retrieval of Interacting Genes (STRING) was employed to construct the PPI networks. Cytoscape (v3.8.2) was visualized to map the selected differential PPI network. The CytoHubba plug-in was used to identify the 10 most important hub genes in the protein interaction network. The colour shade was used to determine the degree algorithm and predict the final score.

Validation by quantitative real-time polymerase chain reaction

The validation of RNA-seq results was performed for four identified miRNAs. The total RNA was isolated from skeletal muscle tissues with an RNA-easy Isolation Reagent (Vazyme Biotech Co., Ltd., Nanjing, China). The miRNA 1st Strand cDNA Synthesis Kit with stem-loop (Vazyme Biotech Co., Ltd.) was used to synthesize miRNA cDNA according to the manufacturer's instructions. Using the software supplied by the

manufacturer (Vazyme Biotech Co., Ltd.), the reverse transcription primers and U6 for miRNAs were designed. A miRNA universal SYBR qPCR master mix (Vazyme Biotech Co., Ltd.) was employed to quantify miRNAs.

Hub genes were validated using qRT-PCR. The cDNA of mRNA was synthesized with a HiScript III 1st Strand cDNA Synthesis Kit (Vazyme Biotech Co., Ltd.). The primers of the genes were designed by Sangon Biotech (Shanghai, China). Taq Pro Universal SYBR qPCR Master Mix (Vazyme Biotech Co., Ltd.) was used for the qRT-PCR of the mRNA. For every sample, 20-µL reactions were executed in triplicate according to the manufacturer's instructions. The cycle for qPCR included three steps. Step 1 involved enzyme activation at 95°C for 30 s (or 5 min for miRNA); Step 2 involved 40 cycles of denaturation at 95°C for 10 s and annealing at 60°C for 30 s; and Step 3 involved one cycle of denaturation at 95°C for 15 s, annealing at 60°C for 60 s and denaturation at 95°C for 15 s.

The StepOnePlus™ System (Applied Biosystems, USA) was employed to perform qRT-PCR analysis on all samples in triplicate. An mRNA endogenous control was provided by GAPDH, whereas a miRNA exogenous control was provided by U6 snRNA. Primer sequences were presented in Supporting Information, *Table S1*. The $2^{-\Delta\Delta CT}$ method was applied on all experimental results.

Western blot

The gastrocnemius muscle samples were prepared by sequentially washing twice with PBS, lysing with a RIPA lysis buffer and homogenizing on ice with a mixture of proteases and phosphatase inhibitor (Biyuntian Biotechnology Co., Ltd., Shanghai, China). The centrifugation was used to separate the homogenate at 15 000 × g for 10 min at 4°C. Total proteins in the homogenate were measured by BCA kit analysis (Walterson Biotechnology Inc., Beijing, China) and denatured by boiling in a water bath at 95°C for 5 min. Sodium dodecyl sulfate-polyacrylamide gel electrophoresis (SDS-PAGE) was used to separate the soluble proteins. The separated proteins were then transferred to a polyvinylidene difluoride (PVDF) membrane. The target protein in the membrane was incubated with primary antibodies against NRAS, MuRF1 and AR (Abcam Inc., Cambridge, MA, USA); BDNF (Wuhan Servicebio Technology Co., Ltd., Wuhan, China); Bcl-2, IGF-I and GAPDH (GeneTex Inc., Irvine, CA, USA); HIF-1 α , FAK, phosphor-NF- κ B p65^{Ser536}, NF- κ B p65, Beclin1, p62, LC3 and Bax (Cell Signaling Technology Inc., Danvers, MA, USA); and the corresponding secondary antibody (Boster Biotech Co., Ltd., Wuhan, China). An ultra-sensitive fluorescence/chemiluminescence imaging system, ChemiScope6300 (CLiNX Science Instruments, Shanghai, China), was employed to visualize the bands with an enhanced chemiluminescence (ECL) reagent.

Statistical analysis

The mean and standard deviation ($M \pm SD$) were calculated for all data. One-way analysis of variance (ANOVA) was used for normally distributed data. Kruskal–Wallis analysis was used in non-parametric distribution through GraphPad Prism 9.0.0 software (GraphPad Software, Inc., La Jolla, CA, USA). A statistically significant difference was considered at P value < 0.05 .

Results

Exercise interventions alleviated the decline of gastrocnemius muscle weight/body weight ratios in aged rats

Previous studies have demonstrated that aging can cause gradual changes in body compositions and a decline in strength and mass of skeletal muscle. As a consequence, skeletal muscle fibres are significantly reduced, especially type II fibres.¹² The gastrocnemius muscle was thus chosen as the experimental object in this study. The GMW/BW ratio was taken as the SI for the indicator of skeletal muscle atrophy.¹¹ Sarcopenia was determined when the SI value of the rats from the aging group was lower than that from the young group and the difference was >2 times SD.¹³ Compared with the YC group, the SI value of the rats from the OC group significantly decreased ($P < 0.001$), with the reduction by 2 times SD. However, the gastrocnemius muscle SI values in the OE, OR and OM groups were significantly higher when compared with that in the OC group ($P < 0.01$, $P < 0.001$, $P < 0.05$; Table 1). Consequently, 24-month-old rats revealed the obvious atrophy of skeletal muscle, and a sarcopenia model using naturally aging rats was successfully established. However, 12-week exercise intervention alleviated the reduction in the SI value of aged rats.

Table 1 The gastrocnemius muscle weight/body weight (GMW/BW) ratios in aged rats ($n = 6$)

Group	Body weight (g)	Gastrocnemius muscle (g)	GMW/BW ratio ($\times 100$)
YC	490.3 \pm 48.74	6.42 \pm 0.43	1.31 \pm 0.04
OC	869.5 \pm 40.33	6.66 \pm 0.61	0.77 \pm 0.05 ^{###}
OE	700.1 \pm 43.00	6.12 \pm 0.55	0.87 \pm 0.06 ^{**}
OR	756.2 \pm 30.64	7.66 \pm 0.47	1.01 \pm 0.03 ^{***}
OM	791.0 \pm 46.50	6.71 \pm 0.33	0.85 \pm 0.05 [*]

Note: All data are presented as mean \pm standard deviation ($M \pm SD$). Abbreviations: OC, old control; OE, old-aerobic exercise; OM, old-mixed exercise; OR, old-resistance exercise; YC, youth control.

^{###} $P < 0.001$ versus YC group.

^{*} $P < 0.05$ versus OC group.

^{**} $P < 0.01$ versus OC group.

^{***} $P < 0.001$ versus OC group.

Exercise interventions suppressed the reduction in cross-sectional area of gastrocnemius muscle fibres in aged rats

In comparison with the YC group, the gastrocnemius muscle fibres of the rats in the OC group demonstrated atrophy or degenerative changes at certain degrees, primarily manifested as the roundedness of skeletal muscle fibres, abnormal centralization and internalization of nuclei (Figure 2A) and the significant reduction in CSA of gastrocnemius muscle fibres ($P < 0.01$; Figure 2B). However, compared with the OC group, polygonal and angular myofibers were observed, and the number of atrophic fibres declined significantly, as well as an enlarged CSA of skeletal muscle fibres in rats from the OE, OM and OR groups was detected ($P < 0.01$, $P < 0.05$). Remarkably, the quantification of CSA for gastrocnemius muscle fibres of the rats from the OC group resulted in a nearly 30% reduction, whereas the mean CSA and fibre size distribution were completely improved to different degrees after exercise interventions (Figure 2B,C). In the OE, OR and OM groups, the proportions of muscle fibres with the CSA larger than $5000 \mu\text{m}^2$ were approximately 42.7%, 51% and 41.8%, with the mean CSA values of 4910, 5099 and $4494 \mu\text{m}^2$, respectively, whereas the proportion of muscle fibres with the CSA larger than $5000 \mu\text{m}^2$ in the OC group was only 15.52%, with the mean CSA value of $3389 \mu\text{m}^2$ (Figure 2B, C), suggesting that exercise interventions can greatly suppress the reduction in CSA and the atrophy of gastrocnemius muscle fibres in aged rats.

Overview of the microRNAs sequencing in aged skeletal muscle

In this study, the raw data and clean data of microRNAs sequencing (miRNA-seq) results for gastrocnemius muscle samples were collected and analysed. RNA-seq analysis demonstrated that Q20 $> 99\%$, Q30 $> 97\%$, and the GC content ratios were in the range of 46–51%. After filtration, the analysis of the length distribution of clean reads indicated that the average lengths of the reads were 21–23 nt, and the reads with the length of 22 nt had the highest population, accounting for approximately half of the total clean reads (Table S2). A total of 965 miRNAs were identified across all samples, including 764 known miRNAs and 201 novel miRNAs. According to miRbase, the known miRNA sequences of species were identified, and the information of 20 known miRNAs with top expression levels in the samples were also summarized (Table S3). Novel miRNA prediction and miRNA quantification were performed using miRDeep2 software. Among them, the highest miRDeep2 score reflected the prediction reliability. The novel miRNAs based on prediction were deemed rno-novel-miR-1 to rno-novel-miR-201 by ‘-’ linking species name abbreviation, ‘novel’, number, ‘mature’

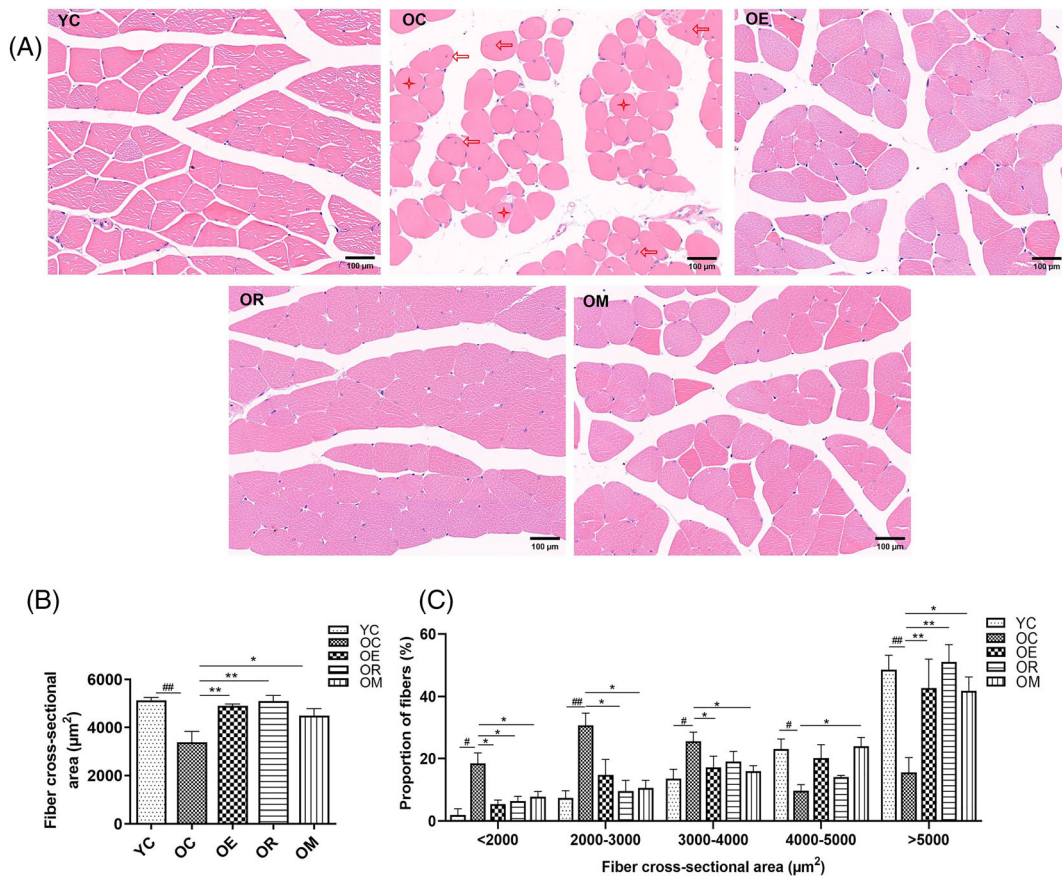


Figure 2 Exercise interventions increased the cross-sectional area (CSA) of skeletal muscle fibres in aged rats. (A) Representative images of skeletal muscle with haematoxylin–eosin staining (scale bar, 100 µm). (B) Average fibre CSA determined from cross-sections of the gastrocnemius muscle. (C) Frequency histograms presenting the distribution of CSA in aged rats. All data were presented as mean \pm standard deviation ($M \pm SD$) ($n = 3$ rats per group). The arrows present nucleus-migrated fibres; asterisks present the roundness of skeletal muscle fibres. $^{##}P < 0.01$ and $^{\#}P < 0.05$ versus YC group; $^{**}P < 0.01$ and $^{*}P < 0.05$ versus OC group. OC, old control; OE, old-aerobic exercise; OM, old-mixed exercise; OR, old-resistance exercise; YC, youth control

or ‘star’ according to the common nomenclature of different species. Similarly, the 20 novel miRNAs with top expression quantity were summarized (Table S3).

Analysis of differentially expressed microRNAs in aged skeletal muscle

The abundance of each mature miRNA was normalized by the total number of miRNA reads in a given library and was scaled to reads per million (RPM). A boxplot was developed to reveal the distribution of the RPM of the samples (Figure S1A). A sample correlation heatmap was designed to analyse the clustering and correlation of the samples (Figure S1B).

There were 13 miRNAs with a significantly differential expression in the OC group when compared with the YC group, and cluster analysis of expression differences was conducted. A heatmap and vertical histogram of the DEMs in each group was designed (Figure 3A,B), with three up-regulated and four down-regulated miRNAs in the OE versus OC group, two

up-regulated miRNAs in the OR versus OC group, six up-regulated and five down-regulated miRNAs in the OM versus OC group (Table S4). Based on these results, different expression patterns of miRNAs could be closely associated with aging and skeletal muscle growth.

Function enrichment analysis

Further analyses were conducted on their target genes to determine whether these DEMs belong to any functional clusters. For the down-regulated genes in the OC versus YC group, the top 10 genes were involved in the biological process, cellular component and molecular function categories. Our results demonstrated that the down-regulated genes were primarily involved in biological processes such as cell cycle, NF- κ B signalling and ubiquitin-dependent protein catabolic processes (Figure S2A). In contrast, after exercise interventions, these down-regulated genes were reversed, with involvement in biological processes such as apoptosis,

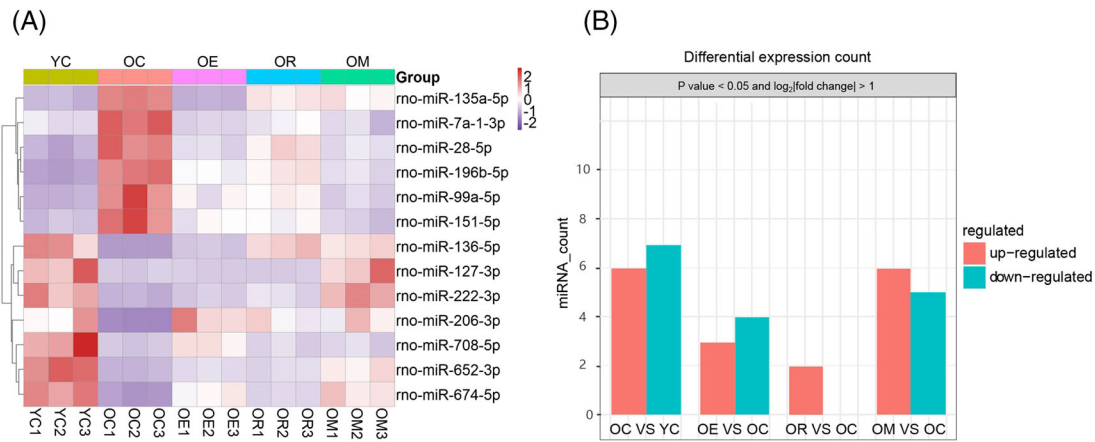


Figure 3 Heatmap (A) and vertical histogram of differentially expressed microRNAs (B) in skeletal muscle of aged rats. OC, old control; OE, old-aerobic exercise; OM, old-mixed exercise; OR, old-resistance exercise; YC, youth control

autophagy, ubiquitin-dependent protein catabolic process, NF- κ B signalling, Wnt signalling, TOR signalling and JNK cascade (Figure 4A). Interestingly, the factors affecting NF- κ B signalling and ubiquitin-dependent protein catabolism were

all involved in the OC, YC and exercise intervention groups. KEGG pathways demonstrated the enrichment of down-regulated genes between the OC and YC groups. Multiple signalling pathways in aged skeletal muscle were

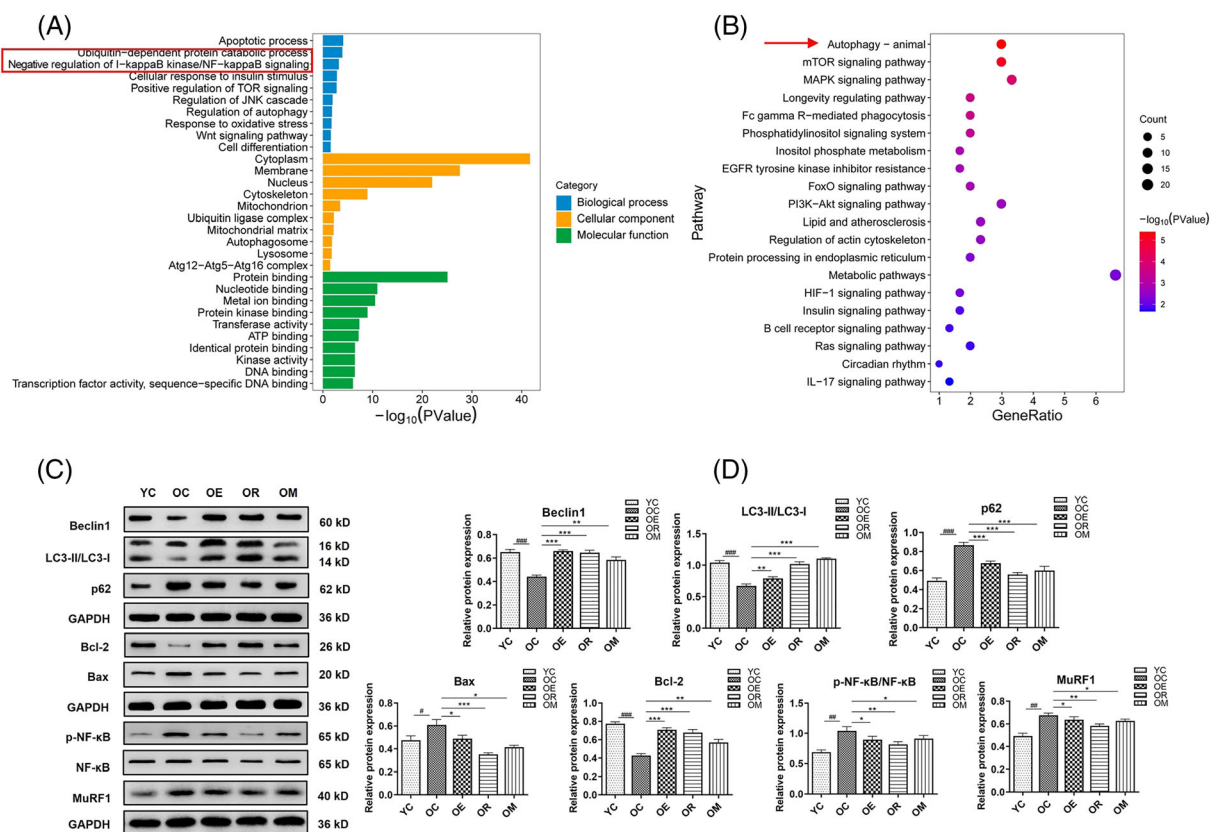


Figure 4 Function enrichment analysis. (A, B) Gene Ontology annotation and Kyoto Encyclopedia of Genes and Genomes enrichment scatter plot of differentially expressed genes. Circle sizes represent gene counts, whereas circle colours indicate P values. (C, D) Western blot validation of biomarker proteins associated with apoptosis, autophagy and the NF- κ B/MuRF1 signal pathways. Equal protein loading was confirmed via GAPDH. All data are presented as mean \pm standard deviation ($M \pm SD$). #### $P < 0.001$, ### $P < 0.01$ and # $P < 0.05$ versus YC group; *** $P < 0.001$, ** $P < 0.01$ and * $P < 0.05$ versus OC group. OC, old control; OE, old-aerobic exercise; OM, old-mixed exercise; OR, old-resistance exercise; YC, youth control

enriched, including mitophagy, insulin secretion, thyroid hormone and the Ras signalling pathway (Figure S2B). Conversely, the KEGG pathway enrichment for the up-regulated genes upon exercise interventions was involved in autophagy, circadian rhythm, actin cytoskeleton, metabolism, mTOR, MAPK, EGFR, FoxO, PI3K/Akt, HIF-1, insulin, Ras and other signalling pathways (Figure 4B).

Following exercise interventions, DEGs enriched in apoptosis, autophagy, NF- κ B and ubiquitin-dependent protein catabolic process might potentially be crucial for sarcopenia (Figure 4C,D). Next, the expression of biomarker proteins involved in three signalling pathways was determined by western blot. The results indicated that, compared with the YC group, the LC3-II/LC3-I ratio and Beclin1 associated with autophagy were significantly down-regulated ($P < 0.001$), whereas p62 was significantly up-regulated in the OC group ($P < 0.001$). In contrast, rats from exercise intervention groups demonstrated a significantly decreased expression of p62 ($P < 0.001$) and a significantly increased expression of Beclin1 ($P < 0.001$, $P < 0.01$), as well as an increased LC3-II/LC3-I ratio ($P < 0.01$, $P < 0.001$) (Figure 4D). Compared with the YC group, the pro-apoptotic biomarker Bax ($P < 0.05$) was significantly up-regulated, and the anti-apoptotic biomarker Bcl-2 ($P < 0.001$) was significantly down-regulated in the OC group. Nevertheless, exercise interventions explicitly attenuated apoptotic cell death, as shown by the significantly decreased expression of Bax ($P < 0.05$, $P < 0.001$) and increased expression of Bcl-2 ($P < 0.001$, $P < 0.01$) in the skeletal muscle from rats undergoing different exercise interventions (Figure 4D). Additionally, the p-NF- κ B/NF- κ B ratio ($P < 0.01$) and MuRF1 ($P < 0.01$) associated with the NF- κ B and ubiquitin-dependent protein catabolic process signalling pathway in sarcopenic rats from the OC group were extraordinarily up-regulated when compared with the YC group. Exercise interventions, on the other hand, significantly reduced the p-NF- κ B/NF- κ B ratio ($P < 0.05$, $P < 0.01$) and the expression of MuRF1 ($P < 0.05$, $P < 0.01$; Figure 4D).

Establishment of protein–protein interaction, miRNA–mRNA interaction network and identification of hub genes

To elucidate the underlying mechanisms of exercise interventions for aging-induced muscular atrophy, the regulation process needs to be further investigated. In this study, the PPI network was established according to the latest STRING database (Figure S3). Subsequently, it was initially identified that these six genes (*Ar*, *Igf1*, *Hif1a*, *Bdnf*, *Fak* and *Nras*) had a strong interaction with a confidence level greater over 0.4 and were likely to be hub genes in aging-induced skeletal muscle atrophy (Figure 6A).

We focused on the 13 miRNAs (corresponding to 505 target genes) highly associated with aging-induced muscular atrophy. The visualization of miRNA–mRNA interactions was depicted (Figures 5A and 54). Multiple miRNAs were up-regulated during the aging process of skeletal muscle, including miR-7a-1-3p, miR-28-5p, miR-99a-5p, miR-135a-5p, miR-151-5p and miR-196b-5p. In contrast, miR-127-3p, miR-136-5p, miR-206-3p, miR-222-3p, miR-652-3p, miR-674-5p and miR-708-5p were down-regulated, which was connected to skeletal muscle function through at least two potential targets. Some of the important hub genes related to skeletal muscle atrophy (*Ar*, *Igf1*, *Hif1a*, *Bdnf*, *Fak* and *Nras*) were targeted by miR-7a-1-3p, miR-135a-5p, miR-151-5p and miR-196b-5p at the core of the miRNA–mRNA network after exercise interventions (Figure 5A). Therefore, miRNAs and their potential target genes may potentially contribute to aging-induced muscular atrophy.

Validation of microRNAs sequencing data and hub genes

The qRT-PCR analysis was performed for four miRNAs and six hub genes to validate their differential expression. As a consequence of aging, the expression of miRNAs such as miR-7a-1-3p, miR-135a-5p, miR-151-5p and miR-196b-5p demonstrated a significant difference between four groups ($P < 0.001$; Figure 5B). Similarly, with an increase in age, exercise interventions rescued the down-regulated hub genes (*Ar*, *Igf1*, *Hif1a*, *Bdnf*, *Fak* and *Nras*) caused by aging ($P < 0.001$, $P < 0.01$; Figure 6B). Each vertical axis indicates the normalized expression levels of miRNAs and hub genes. Based on the expression level and sequencing abundance of skeletal muscle from the OC group, a control set of miRNAs was developed on a scale of 1. Therefore, miRNA expression levels determined by qRT-PCR agreed with miRNA-seq data, thus demonstrating their accuracy ($P < 0.001$; Figure 5C).

Furthermore, the roles of AR, IGF1, HIF1A, BDNF, FAK and NRAS in sarcopenia have not been reported. Therefore, the proteins in the gastrocnemius muscle were selected for western blot analysis, which verified that exercise interventions effectively suppressed the down-regulation of AR, IGF1, HIF1A, BDNF, FAK and NRAS expression in aging-related muscular dystrophy at the protein level ($P < 0.001$, $P < 0.01$; Figure 6C,D).

Discussion

Currently, multiple models have been utilized to explore aging-related skeletal muscle atrophy. Compared with the drug- or surgery-induced aging models, the naturally aging model can accurately represent the characteristics of human

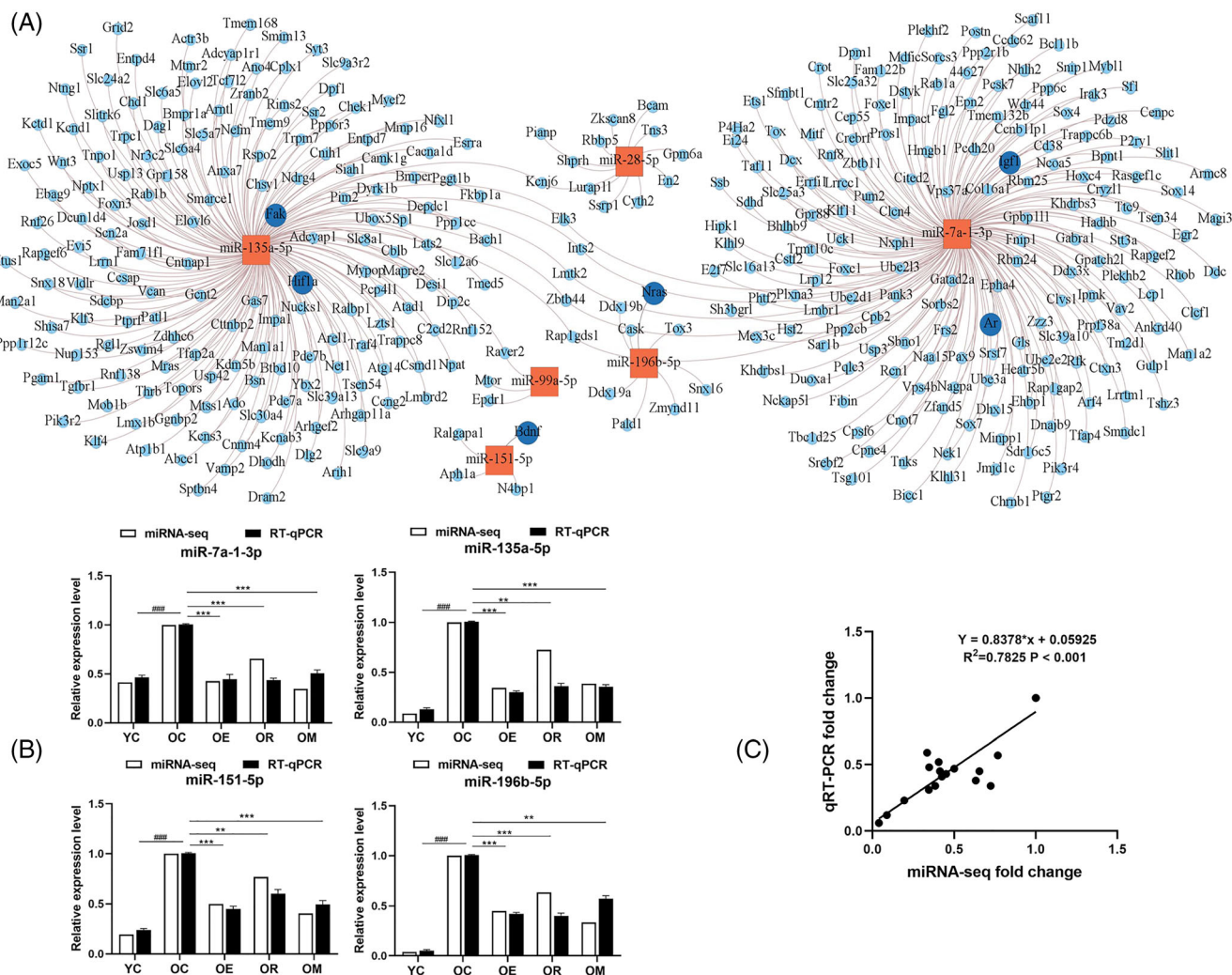


Figure 5 Validation of microRNA sequencing (miRNA-seq) data and differentially expressed miRNAs (DEMs) in aged skeletal muscle. (A) The visualization of miRNA–mRNA interaction network associated with sarcopenia. Up-regulated miRNAs or genes are shown in blue; and down-regulated miRNAs or genes are shown in red. (B) The relative expression levels of six DEMs, including miR-7a-1-3p, miR-135a-5p, miR-151-5p and miR-196b-5p, were determined by quantitative real-time polymerase chain reaction (qRT-PCR) with the normalization against U6. The expression levels and sequencing abundance of miRNAs in the skeletal muscle of the rats from the OC group were set to 1 for each miRNA. (C) Correlation analysis between the relative expression and miRNA-seq results of four DEMs. R^2 : correlation coefficient; Pearson correlation coefficient with $P < 0.001$. All data are presented as mean \pm standard deviation (M \pm SD). $####P < 0.001$ versus YC group; $***P < 0.001$ and $**P < 0.01$ versus OC group. OC, old control; OE, old-aerobic exercise; OM, old-mixed exercise; OR, old-resistance exercise; YC, youth control

aging and is safe, reliable and reproducible. Therefore, the experimental result should be more realistic. Meanwhile, Wistar rats were used in various studies to represent an aging model, and their life expectancy was approximately 2.5–3 years.¹⁴ At the end of the exercise interventions in this experiment, the rats were 24 months old, reaching up to 80% of their average lifespan. Concurrently, a visual inspection of the rats revealed obvious aging signs such as messy and withered fur and severe hair loss. This confirms that the naturally aging rat model in this study was successfully constructed.¹⁵ Notably, the significantly decreased SI values and CSA of these aged rats, as well as a series of histological manifestations of skeletal muscle fibre atrophy, including the roundness of

skeletal muscle fibres and the centralization of nuclei, were observed, which suggests the successful establishment of real sarcopenia during the natural aging process.¹⁶ Exercise intervention has been proven to be one of the best approaches to maintain and enhance skeletal muscle mass and strength and to prevent and treat sarcopenia.¹⁷ Resistance exercise can effectively promote protein synthesis in skeletal muscle, and aerobic exercise can significantly improve mitochondrial function and aerobic capacity. In both strategies, skeletal muscle with strong endurance capacity can be developed, and its energy metabolism can be improved.¹⁸ Based on the results obtained, various exercise intervention modes could alleviate aging-induced skeletal muscle atrophy, as validated by CSA,

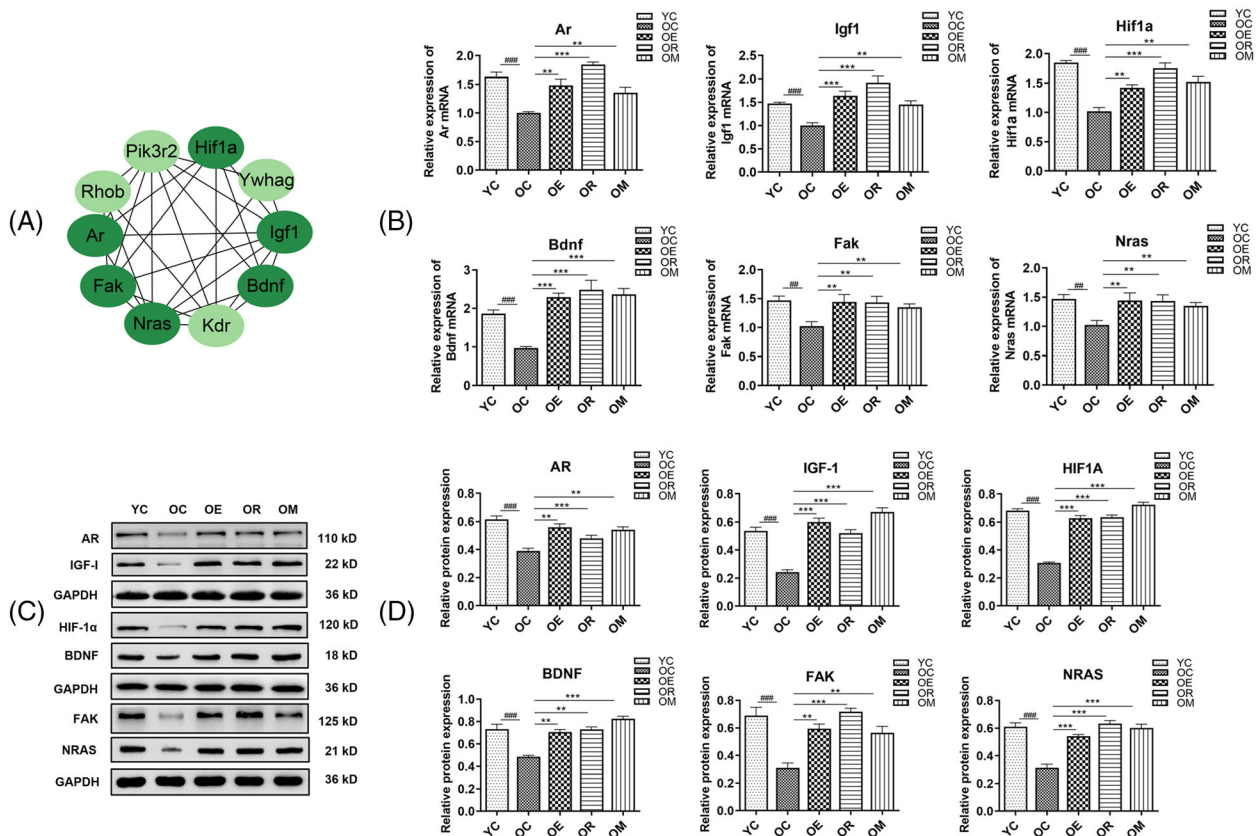


Figure 6 Validation of six hub genes in aged skeletal muscle. (A) Hub genes. (B) The expression levels of six hub genes, namely, Ar, Igf1, Hif1a, Bdnf, Fak and Nras, were normalized against GAPDH. As a control, the expression level in the OC group was set to 1. (C, D) The biomarker proteins were evaluated by western blot. Equal protein loading was normalized by GAPDH. All data are presented as mean \pm standard deviation ($M \pm SD$). $^{####}P < 0.001$ and $^{###}P < 0.01$ versus YC group; $^{***}P < 0.001$ and $^{**}P < 0.01$ versus OC group. OC, old control; OE, old-aerobic exercise; OM, old-mixed exercise; OR, old-resistance exercise; YC, youth control

the most intuitive criterion for skeletal muscle atrophy. This indicates that 12-week exercise interventions could effectively delay skeletal muscle atrophy in naturally aging rats.

After comparing the miRNA profiles in aging skeletal muscle tissues with various exercise interventions, several signal pathways regulated by DEMs were identified. A significant enrichment in apoptosis, autophagy, the NF- κ B/MuRF1 and other signalling pathways was observed. Previous studies demonstrated that autophagy signalling pathways maintain cellular homeostasis and control skeletal muscle mass during aging process.^{19,20} Various exercise modes can up-regulate Beclin1 and LC3-II/LC3-I ratios and down-regulate p62, suggesting that exercise can enhance autophagic flux and facilitate the removal of intracellular damaged proteins and metabolic waste from skeletal muscle fibres.²¹ With increasing age, the pro-apoptotic protein Bax becomes imbalanced with the anti-apoptotic protein Bcl-2, thus leading to protein degradation and apoptosis of skeletal muscle cells.²² As a consequence of up-regulated Bcl-2 and down-regulated Bax in the skeletal muscle of aged rats, exercise intervention

can effectively mitigate the degree of apoptosis. In skeletal muscle, aging is assumed to contribute to the activation of MuRF1 and apoptosis-mediated degradation, thus leading to increased protein degradation.²³ MuRF1 and MAFbx are two ubiquitin E3 ligases specifically expressed in atrophic skeletal muscle.²⁴ Additionally, NF- κ B is a crucial transcriptional regulator that induces the expression of MAFbx and MuRF1, thus activating the process of protein ubiquitination in skeletal muscle atrophy.²⁵ GO analysis revealed that NF- κ B signalling interacts with ubiquitin-dependent protein catabolism, and both are up-regulated by aging and down-regulated by exercise. According to this study, aging can activate the NF- κ B signal pathway, thus increasing MuRF1 transcription, which then results in increased protein degradation. Additionally, followed by exercise, NF- κ B-mediated MuRF1 expression was reduced in sarcopenic muscle, and the aging-associated activation of catabolic signalling was inhibited, thus delaying muscular atrophy. The potential mechanisms associated with above signal pathways in skeletal muscle atrophy were confirmed in this study. This allows

for an important reference to explain the regulatory pathways of exercise intervention and to prevent and treat sarcopenia.

This study investigated the miRNA–mRNA network associated with aging-related muscular atrophy. miR-7a-1-3p, miR-135a-5p, miR-151-5p and miR-196b-5p were at the core of the miRNA–mRNA network with the down-regulation and were associated with aging-induced muscular atrophy upon exercise interventions. In the network, the key nodes comprised Ar, Igf1, Hif1a, Bdnf, Fak and Nras.

In these node genes, Ar acts as a biological macromolecule for mediating androgen action. An androgen receptor complex can be formed between androgen and Ar, which then promote the proliferation and differentiation of satellite cells in skeletal muscle, thus enhancing protein synthesis.²⁶ Additionally, androgen also has adipogenic effects, primarily because it can inhibit the adipogenic differentiation of multipotent mesenchymal stem cells and promote their commitment to the myogenic lineage.²⁷ Therefore, low androgen is often associated with body weight loss, muscle atrophy and increased body fat percentage. Ar is altered in skeletal muscle following exercise-induced morphological and functional changes. In agreement with other studies, our results revealed that various exercise interventions can stimulate the expression of Ar mRNA and protein in skeletal muscle.²⁸ Another important node gene, insulin-like growth factor 1 (IGF-1), promotes the proliferation and differentiation of myogenic cells, as well as protein synthesis, in skeletal muscle.²⁹ In previous studies, the IGF-1/Akt/mTOR signalling pathway was associated with skeletal muscle hypertrophy.³⁰ Meanwhile, the overexpression of IGF-1 also inhibits FoxO-mediated MAFbx and MuRF1 in the ubiquitin-mediated proteasome system, thus inhibiting protein degradation and rescuing skeletal muscle atrophy.³¹ One study confirmed that progressive resistance training can reverse the aging-induced down-regulation of IGF-1 in skeletal muscle.³² With increasing age, miR-7a-1-3p was up-regulated, thus inhibiting the expression of the target genes Ar and Igf1, whereas exercise increased the expression of Ar and Igf1 and promoted cell proliferation and protein synthesis in skeletal muscle.

Moreover, miR-135a-5p, which has been found to be down-regulated, may have a key role in the modulation of skeletal muscle strength by regulating the protein tyrosine kinase 2 (Ptk2, FAK). As a mechanosensitive or exercise-responsive protein, FAK has a vital role in the morphology, metabolism and insulin sensitivity of skeletal muscle.³³ A decline in skeletal muscle stem cell regeneration is associated with impaired FAK signalling during aging.³⁴ Nevertheless, few studies explored the effects of exercise on FAK. Additionally, the polymorphism of hypoxia-inducible factor 1 α (HIF-1 α), associated with an increase in fast fibres by 50% in skeletal muscle, is common among strength athletes.³⁵ When exercise causes oxygen deficiency, HIF-1 α degrades less and accumulates continuously, which is the

most critical protein involved in oxygen transport and utilization during exercise.³⁶ Interestingly, oxygen consumption and oxidative stress in the mitochondria of skeletal muscle from mice decreased under hypoxia, thus improving overall cell survival. The reduction of HIF-1 α can lead to an increase in reactive oxygen species (ROS), and the accumulation of HIF-1 α plays a positive role in reducing oxidative stress.³⁷ Our previous studies have demonstrated that aging leads to increased oxidative stress, which in turn triggers apoptosis and skeletal muscle atrophy.²¹

The BDNF gene, whose expression is controlled by miR-151-5p, also has modified transcription levels associated with neurobiology and metabolism in skeletal muscle. In response to skeletal muscle injury, BDNF enhances satellite cell activation and proliferation, thus implying that BDNF may be critical in mediating satellite cell responses to skeletal muscle injury.³⁸ The overexpression of BDNF was associated with the expression of genes related to fast-twitch muscle and the number of glycolytic fibres. In contrast, this alters the proportion of various types of muscle fibres and decreases motor endplate volume.³⁹ At the same time, muscle mass and muscle fibre CSA increase are correlated with BDNF level in skeletal muscle.⁴⁰ Consequently, BDNF may affect the development and progression of sarcopenia by modulating the neuromuscular function during the aging process.

Furthermore, the Ras gene is encoded by proto-oncogenes, including K, N and H types, and primarily affects the proliferation and differentiation of cells by participating in regulating the MAPK (ERK1/2) signalling pathway. One previous study has demonstrated that apoptosis is significantly induced when N-Ras is knocked down during differentiation. N-Ras can protect cells against apoptosis by increasing the ratio of Bcl-2 to Bax.⁴¹ Isoform-specific knockout experiments demonstrate that skeletal muscle differentiation is directly affected by H-Ras and K-Ras, whereas N-Ras has a vital role in preserving cell survival by acting as an anti-apoptotic protein.⁴² According to the results obtained in this study, down-regulating miR-196b-5p may enhance N-Ras expression in aging skeletal muscle, thus reducing apoptosis. Therefore, based on the interaction network described above, several miRNAs and hub genes may have a critical role in the posttranscriptional regulation of aging-induced muscular dystrophy.

Conclusion

The comprehensive analysis of the miRNA profile in the skeletal muscle of the aged rats upon exercise interventions allows for the identification of DEMs and hub genes that are potentially associated with aging-induced muscular atrophy. Our identified key miRNAs (miR-7a-1-3p, miR-135a-5p, miR-151-5p and miR-196b-5p) and hub genes (Ar, Igf1, Hif1a,

Bdnf, Fak and Nras) could be the potential targets for regulating sarcopenia. The close relationship between miRNAs and hub genes identified in this study, as well as aging skeletal muscle and the interesting molecular signal pathways and biological processes, is crucial to alleviate and treat aging-induced muscle atrophy through exercise interventions. Furthermore, the presented miRNA–mRNA network analysis offers an essential reference for the accurate or non-invasive prediction, diagnosis, development and evaluation of exercise intervention strategies, as well as for monitoring intervention efficiency for sarcopenia.

Acknowledgements

The authors of this manuscript certify that they complied with the ethical guidelines for authorship and publishing in the *Journal of Cachexia, Sarcopenia and Muscle*.⁴³

Conflict of interest

The authors declare no conflict of interest.

References

- Cruz-Jentoft AJ, Baeyens JP, Bauer JM, Boirie Y, Cederholm T, Landi F, et al. Sarcopenia: European consensus on definition and diagnosis: report of the European Working Group on Sarcopenia in Older People. *Age Ageing* 2010;**39**:412–423.
- Rosenberg IH. Sarcopenia: origins and clinical relevance. *J Nutr* 1997;**127**:990s–991s.
- Cruz-Jentoft AJ, Sayer AA. Sarcopenia. *Lancet (London, England)* 2019;**393**:2636–2646.
- Suzuki T, Springer J. MicroRNAs in muscle wasting. *J Cachexia Sarcopenia Muscle* 2018;**9**:1209–1212.
- McCormick R, Goljanek-Whysall K. MicroRNA dysregulation in aging and pathologies of the skeletal muscle. *Int Rev Cell Mol Biol* 2017;**334**:265–308.
- Shur NF, Creedon L, Skirrow S, Atherton PJ, MacDonald IA, Lund J, et al. Age-related changes in muscle architecture and metabolism in humans: the likely contribution of physical inactivity to age-related functional decline. *Ageing Res Rev* 2021;**68**:101344.
- McGregor RA, Poppitt SD, Cameron-Smith D. Role of microRNAs in the age-related changes in skeletal muscle and diet or exercise interventions to promote healthy aging in humans. *Ageing Res Rev* 2014;**17**:25–33.
- Javanmardifard Z, Shahrbanian S, Mowla SJ. MicroRNAs associated with signaling pathways and exercise adaptation in sarcopenia. *Life Sci* 2021;**285**:119926.
- Bedford TG, Tipton CM, Wilson NC, Oppliger RA, Gisolfi CV. Maximum oxygen consumption of rats and its changes with various experimental procedures. *J Appl Physiol Respir Environ Exerc Physiol* 1979;**47**:1278–1283.
- Aamann L, Ochoa-Sanchez R, Oliveira M, Tremblay M, Bémeur C, Dam G, et al. Progressive resistance training prevents loss of muscle mass and strength in bile duct-ligated rats. *Liver international: official journal of the International Association for the Study of the Liver* 2019;**39**:676–683.
- Edström E, Ulfhake B. Sarcopenia is not due to lack of regenerative drive in senescent skeletal muscle. *Ageing Cell* 2005;**4**:65–77.
- Nilwik R, Snijders T, Leenders M, Groen BB, van Kranenburg J, Verdijk LB, et al. The decline in skeletal muscle mass with aging is mainly attributed to a reduction in type II muscle fiber size. *Exp Gerontol* 2013;**48**:492–498.
- Baumgartner RN, Koehler KM, Gallagher D, Romero L, Heymsfield SB, Ross RR, et al. Epidemiology of sarcopenia among the elderly in New Mexico. *Am J Epidemiol* 1998;**147**:755–763.
- Ghasemi A, Jeddi S, Kashfi K. The laboratory rat: age and body weight matter. *EXCLI J* 2021;**20**:1431–1445.
- Zhou M, Yuan Y, Lin Z, Zhang B, Qin W, Liu Y, et al. Acupoint catgut embedding improves senescence in a rat model of ageing by regulating mitophagy via the PINK1 pathway. *J Cell Mol Med* 2021;**25**:3816–3828.
- Sayed RK, de Leonardis EC, Guerrero-Martínez JA, Rahim I, Mokhtar DM, Saleh AM, et al. Identification of morphological markers of sarcopenia at early stage of aging in skeletal muscle of mice. *Exp Gerontol* 2016;**83**:22–30.
- Landi F, Marzetti E, Martone AM, Bernabei R, Onder G. Exercise as a remedy for sarcopenia. *Curr Opin Clin Nutr Metab Care* 2014;**17**:25–31.
- SPRINTT Consortium, Marzetti E, Calvani R, Tosato M, Cesari M, di Bari M, et al. Physical activity and exercise as countermeasures to physical frailty and sarcopenia. *Ageing Clin Exp Res* 2017;**29**:35–42.
- Carter HN, Kim Y, Erlich AT, Zarrin-Khat D, Hood DA. Autophagy and mitophagy flux in young and aged skeletal muscle following chronic contractile activity. *J Physiol* 2018;**596**:3567–3584.
- García-Prat L, Martínez-Vicente M, Perdiguer E, Ortet L, Rodríguez-Ubreva J, Rebollo E, et al. Autophagy maintains stemness by preventing senescence. *Nature* 2016;**529**:37–42.
- Liang J, Zhang H, Zeng Z, Wu L, Zhang Y, Guo Y, et al. Lifelong aerobic exercise alleviates sarcopenia by activating autophagy and inhibiting protein degradation via the AMPK/PGC-1 α signaling pathway. *Metabolites* 2021;**11**:323.

Funding

This work was supported by the National Natural Science Foundation of China (Nos 32071176, 31571228), the Key Special Project of Disciplinary Development, Hubei Superior Discipline Groups of Physical Education and Health Promotion from Hubei Provincial Department of Education, the 14th Five-Year-Plan Advantageous and Characteristic Disciplines (Groups) of Colleges and Universities in Hubei Province from Hubei Provincial Department of Education and the Chutian Scholar Program and Innovative Start-Up Foundation from Wuhan Sports University to NC; as well as the Youth Scientific and Research Team from Wuhan Sports University (No. 21KT08) and the Science and Technology Research Project from Education Department of Hubei Province (No. Q20194102) to JF.

Online supplementary material

Additional supporting information may be found online in the Supporting Information section at the end of the article.

22. Dupont-Versteegden EE. Apoptosis in skeletal muscle and its relevance to atrophy. *World J Gastroenterol* 2006;**12**: 7463–7466.
23. Marzetti E, Calvani R, Bernabei R, Leeuwenburgh C. Apoptosis in skeletal myocytes: a potential target for interventions against sarcopenia and physical frailty—a mini-review. *Gerontology* 2012; **58**:99–106.
24. Rom O, Reznick AZ. The role of E3 ubiquitin-ligases MuRF-1 and MAFbx in loss of skeletal muscle mass. *Free Radic Biol Med* 2016;**98**:218–230.
25. Bodine SC, Baehr LM. Skeletal muscle atrophy and the E3 ubiquitin ligases MuRF1 and MAFbx/atrogen-1. *Am J Physiol Endocrinol Metab* 2014;**307**:E469–E484.
26. Rossetti ML, Steiner JL, Gordon BS. Androgen-mediated regulation of skeletal muscle protein balance. *Mol Cell Endocrinol* 2017; **447**:35–44.
27. Singh R, Artaza JN, Taylor WE, Gonzalez-Cadavid NF, Bhasin S. Androgens stimulate myogenic differentiation and inhibit adipogenesis in C3H 10T1/2 pluripotent cells through an androgen receptor-mediated pathway. *Endocrinology* 2003;**144**: 5081–5088.
28. Willoughby DS, Taylor L. Effects of sequential bouts of resistance exercise on androgen receptor expression. *Med Sci Sports Exerc* 2004;**36**:1499–1506.
29. Clemmons DR. Role of IGF-I in skeletal muscle mass maintenance. *Trends Endocrinol Metab* 2009;**20**:349–356.
30. Rommel C, Bodine SC, Clarke BA, Rossman R, Nunez L, Stitt TN, et al. Mediation of IGF-1-induced skeletal myotube hypertrophy by PI(3)K/Akt/mTOR and PI(3)K/Akt/GSK3 pathways. *Nat Cell Biol* 2001;**3**:1009–1013.
31. Glass DJ. Skeletal muscle hypertrophy and atrophy signaling pathways. *Int J Biochem Cell Biol* 2005;**37**:1974–1984.
32. Urso ML, Fiatarone Singh MA, Ding W, Evans WJ, Cosmas AC, Manfredi TG. Exercise training effects on skeletal muscle plasticity and IGF-1 receptors in frail elders. *Age (Dordr)* 2005;**27**:117–125.
33. Luca E, Turcekova K, Hartung A, Mathes S, Rehrauer H, Krützfeldt J. Genetic deletion of microRNA biogenesis in muscle cells reveals a hierarchical non-clustered network that controls focal adhesion signaling during muscle regeneration. *Mol Metab* 2020;**36**:100967.
34. Lukjanenko L, Jung MJ, Hegde N, Perruisseau-Carrier C, Migliavacca E, Roza M, et al. Loss of fibronectin from the aged stem cell niche affects the regenerative capacity of skeletal muscle in mice. *Nat Med* 2016;**22**:897–905.
35. Lunde IG, Anton SL, Bruusgaard JC, Rana ZA, Ellefsen S, Gundersen K. Hypoxia inducible factor 1 links fast-patterned muscle activity and fast muscle phenotype in rats. *J Physiol* 2011;**589**:1443–1454.
36. Freyssenet D. Energy sensing and regulation of gene expression in skeletal muscle. *J Appl Physiol* 1985;**2007**:529–540.
37. Kim JW, Tchernyshyov I, Semenza GL, Dang CV. HIF-1-mediated expression of pyruvate dehydrogenase kinase: a metabolic switch required for cellular adaptation to hypoxia. *Cell Metab* 2006;**3**:177–185.
38. Clow C, Jasmin BJ. Brain-derived neurotrophic factor regulates satellite cell differentiation and skeletal muscle regeneration. *Mol Biol Cell* 2010;**21**:2182–2190.
39. Guilherme J, Semenova EA, Borisov OV, Kostryukova ES, Vepkhvadze TF, Lysenko EA, et al. The BDNF-increasing allele is associated with increased proportion of fast-twitch muscle fibers, handgrip strength, and power athlete status. *J Strength Cond Res* 2022;**36**:1884–1889.
40. Yarrow JF, White LJ, McCoy SC, Borst SE. Training augments resistance exercise induced elevation of circulating brain derived neurotrophic factor (BDNF). *Neurosci Lett* 2010;**479**:161–165.
41. Castellano E, De Las RJ, Guerrero C, Santos E. Transcriptional networks of knockout cell lines identify functional specificities of H-Ras and N-Ras: significant involvement of N-Ras in biotic and defense responses. *Oncogene* 2007;**26**: 917–933.
42. Lee J, Choi KJ, Lim MJ, Hong F, Choi TG, Tak E, et al. Proto-oncogenic H-Ras, K-Ras, and N-Ras are involved in muscle differentiation via phosphatidylinositol 3-kinase. *Cell Res* 2010;**20**:919–934.
43. von Haehling S, Morley JE, Coats AJS, Anker SD. Ethical guidelines for publishing in the Journal of Cachexia, Sarcopenia and Muscle: update 2021. *J Cachexia Sarcopenia Muscle* 2021;**12**:2259–2261.